Gondwana Research 27 (2015) 1574–1585

Contents lists available at ScienceDirect

Gondwana Research

journal homepage: www.elsevier.com/locate/gr

Mesozoic–Cenozoic mantle evolution beneath the North China Craton: A new perspective from Hf–Nd isotopes of basalts

Fanxue Meng [a,b,*], Shan Gao [b], Yaoling Niu [a,c], Yongsheng Liu [b], Xiaorui Wang [b]

[a] Institute of Oceanology, Chinese Academy of Sciences, Qingdao 266071, China
[b] State Key Laboratory of Geological Processes and Mineral Resources, China University of Geosciences, Wuhan 430074, China
[c] Department of Earth Sciences, Durham University, DH1 3LE, UK

ARTICLE INFO

Article history:
Received 31 July 2013
Received in revised form 3 January 2014
Accepted 21 January 2014
Available online 28 February 2014

Handling Editor: G.C. Zhao

Keywords:
Whole-rock Hf isotopes
Mesozoic–Cenozoic basalts
North China Craton

ABSTRACT

We report here the whole-rock Hf–Nd isotopic data on Mesozoic–Cenozoic basaltic lavas from Liaoning, Shandong, Hebei and Jiangsu–Anhui regions in the North China Craton (NCC). These lavas can be readily subdivided into two groups. The older (>110 Ma) lavas are relatively depleted in high field strength elements (HFSEs), and have enriched Sr–Nd–Hf isotopic compositions. The younger (<110 Ma) lavas, by contrast, have OIB-like trace element systematics and more depleted Sr–Nd–Hf isotopic compositions. Among several possibilities, the most straightforward explanation is that the >110 Ma lavas may have largely derived from the "ancient metasomatized lithosphere" or contain contributions from ancient continental crust in the process of lithosphere thinning, whereas the <110 Ma lavas with more depleted Sr–Nd–Hf isotopic compositions were most likely derived from the asthenosphere when the lithosphere had already been thinned with the ancient lithospheric mantle being removed. We thus propose that the thinning of the ancient cratonic mantle lithosphere beneath the NCC must have been largely completed by ~110 Ma. In this context, we infer that ancient sub-continental lithospheric material, once entering the asthenosphere, may be important as an enriched component for intra-plate basaltic magmatism, including ocean island basalts (OIBs). In addition, all these basaltic lavas plot along the terrestrial array in the Hf–Nd isotopic space, suggesting that the mantle source isotopic variation is largely controlled by simple magmatic processes, i.e., low-degree melt metasomatic enrichment (e.g., elevated Hf/Lu and Nd/Sm ratios) and melt extraction-related depletion (e.g., lowered Hf/Lu and Nd/Sm ratios).

1. Introduction

The ancient, cratonic mantle lithosphere of the North China Craton (NCC) is widely thought to have been thinned from the Late Mesozoic through to the Cenozoic in response to some form of thermo-tectonic activities (Menzies et al., 1993; Griffin et al., 1998; Fan et al., 2000; Xu, 2001; Gao et al., 2002; Wu et al., 2003; Gao et al., 2004; Rudnick et al., 2004; Wu et al., 2005, 2006; Menzies et al., 2007; Zhang et al., 2007; Zheng et al., 2007; D.B. Yang et al., 2008; J.H. Yang et al., 2008; W.L. Xu et al., 2008; Y.G. Xu et al., 2008; H.F. Zhang et al., 2009; J.J. Zhang et al., 2009; Xu et al., 2010; Zhang et al., 2011; Zhang, 2012). The occurrence of the Ordovician diamondiferous kimberlite pipes in the NCC indicates the existence of cold and thick (>200 km) lithospheric mantle, typical of Archean cratons, at least at the time of kimberlite eruption in the Paleozoic (Menzies et al., 1993; Griffin et al., 1998). The refractory garnet peridotite xenoliths in the kimberlites give Archean Os model ages, consistent with the geology that both the crust and the mantle lithosphere underlying the NCC are of Archean age (e.g., Gao et al., 2002; Wu et al., 2006; Zhang et al., 2008). Geophysical data and studies of mantle xenoliths from the Cenozoic basalts, however, suggest that the present-day lithosphere is only 60–80 km thick (Menzies et al., 1993; Griffin et al., 1998; Menzies and Xu, 1998; Fan et al., 2000; Zheng et al., 2001; Rudnick et al., 2004; H.F. Zhang et al., 2009). Also, the Cenozoic basalts carry mantle xenoliths that are equilibrated to a high geotherm (Xu, 2001; Zheng et al., 2006), have a relatively fertile bulk composition (Menzies et al., 1993; Griffin et al., 1998; Rudnick et al., 2004) and Os isotopic compositions similar to the modern convective mantle (Gao et al., 2002; Wu et al., 2003; Wu et al., 2006).

The above observations have been used to suggest that the ancient, cratonic mantle lithosphere, similar to that present beneath the Kaapvaal, Siberian and other Archean cratons, was removed from the base of the Eastern Block of the NCC in the Mesozoic, and was partly replenished with younger, less refractory lithospheric mantle (Menzies et al., 1993; Griffin et al., 1998; Fan et al., 2000; Xu, 2001; Gao et al., 2002; Wu et al., 2003; Gao et al., 2004; Rudnick et al., 2004; Wu et al., 2005, 2006; Menzies et al., 2007; Zhang et al., 2007; Zheng et al., 2007; D.B. Yang et al., 2008; J.H. Yang et al., 2008; W.L. Xu et al., 2008; Y.G. Xu et al., 2008; H.F. Zhang et al., 2009; J.J. Zhang et al., 2009; Xu et al., 2010; Zhang et al., 2011; Zhang, 2012). However, the mechanism and actual timing of the thinning remain controversial

* Corresponding author at: Institute of Oceanology, Chinese Academy of Sciences, Qingdao 266071, China. Tel.: +86 18954281119.
E-mail address: mfx1117@163.com (F. Meng).

http://dx.doi.org/10.1016/j.gr.2014.01.014
1342-937X/

(Xu, 2001; Gao et al., 2004; Wu et al., 2005; Menzies et al., 2007; Zhang et al., 2007; Zheng et al., 2007; D.B. Yang et al., 2008; J.H. Yang et al., 2008; W.L. Xu et al., 2008; H.F. Zhang et al., 2009; J.J. Zhang et al., 2009; Xu et al., 2010; Zhang et al., 2011; Zhang, 2012). The major hypotheses include delamination (Deng et al., 1994; Wu et al., 2003; Deng et al., 2004; Gao et al., 2004; Deng et al., 2007; Gao et al., 2008; Ling et al., 2009; Xu et al., 2013), thermo-chemical replacement (Xu, 1999; Zheng, 1999; Lu et al., 2000; Xu, 2001, 2007; Zheng, 2009) and basal hydration weakening (Niu, 2005). The thinning is proposed to be mainly occurred 1) in the Mesozoic (e.g., Zhou et al., 2002; Wu et al., 2003; Zhang et al., 2005; Zhou, 2006, 2009); 2) in the Cenozoic (Menzies et al., 1993; Griffin et al., 1998; Lu et al., 2000; Xu, 2001) and 3) in two stages, respectively, in the Mesozoic and Cenozoic (e.g., Deng et al., 1996, 2004). However, most researchers agree that the peak period of thinning took place at 130–110 Ma (e.g., Zhou et al., 2002; Wilde et al., 2003; Zhai et al., 2005; Zhang et al., 2005; Xu et al., 2009).

Basalts of Mesozoic age are widespread in eastern China and are interpreted as resulting from the lithospheric thinning (Zhang et al., 2002; Zhang and Zheng, 2003; Zhang et al., 2003, 2004; Yang et al., 2006; Gao et al., 2008; Y.S. Liu et al., 2008). Cenozoic basalts of varying age are also abundant in this region. These basalts and mantle xenoliths they carry provide a window into mantle sources and processes. There has been much research on the petrology and geochemistry of these rocks, including Sr–Nd–Pb isotope analysis (Zhang et al., 2002; Zhang and Zheng, 2003; Zhang et al., 2003, 2004; Tang et al., 2006; Huang et al., 2007; Gao et al., 2008; Y.S. Liu et al., 2008; Yang and Li, 2008; J.J. Zhang et al., 2009; Xu et al., 2010; Wang et al., 2011; W. Yang et al., 2012), yet there has been rare Hf isotope study on the NCC basalts (Yang et al., 2006; Chen et al., 2009; Zeng et al., 2011). Hf and Nd isotopes are different between lithospheric mantle and asthenospheric mantle (Griffin et al., 2000), which are powerful in tracing the source of basalts. However, because of $D_{Lu}/D_{Hf} > D_{Sm}/D_{Nd}$, Lu–Hf isotopic system is more sensitive to mineralogy in the source and melting residues during partial melting (Johnson et al., 1996; Vervoort and Patchett, 1996; Schmitz et al., 2004), implying that a significant fractionation of Lu/Hf ratio can occur, which therefore can generate a broad range of Hf isotopic variation (e.g., Yang et al., 2006) and could better trace the source and source histories. In addition, the nature of the source of Cenozoic basalts in the NCC is controversial. Garnet ($D_{Lu} \gg 1$ and $D_{Hf} < 1$) as a residual phase will lead to high Lu/Hf ratios in the melting residue and high $^{176}Hf/^{177}Hf$ ratios relative to $^{143}Nd/^{144}Nd$ (i.e., decoupling), which might be an important tracer for the recycled eclogitic lower crust (Chen et al., 2009; Zeng et al., 2011). However, the Hf and Nd isotopes in this study are coupled. Here, we present high quality whole-rock Hf isotopic data on several suites of representative Mesozoic–Cenozoic basaltic samples from the NCC. Our results indicate that Hf isotopic compositions of basaltic lavas change abruptly from >110 Ma to <110 Ma. The >110 Ma lavas have enriched Hf isotopic compositions. The <110 Ma lavas, by contrast, have more depleted Hf isotopic compositions. Previous studies indicated that there is also an abrupt change in the Sr–Nd–Pb–Mg isotope data (Xu, 2001; Zhang et al., 2002, 2003; Yang and Li, 2008; J.J. Zhang et al., 2009; Xu et al., 2010; W. Yang et al., 2012) and trace element data (e.g., Y.S. Liu et al., 2008) between basalts erupted before 120 Ma and those erupted after 110 Ma. The new Hf isotope data, together with the existing Sr–Nd isotope data and trace element data, offer us new constrains on the petrogenesis of these rocks and insights into the process of lithosphere thinning beneath the NCC.

2. Geological settings and samples

The NCC (Fig. 1) is one of the world's oldest Archean cratons, preserving crustal remnants as old as 3800 Ma (Liu et al., 1992; Song et al., 1996; Liu et al., 2007; D.Y. Liu et al., 2008). It is surrounded by the Mesozoic Dabie and Sulu Orogenic belts to the south and east (Li et al., 1993; Meng and Zhang, 2000), and to the north by the Central Asian Orogenic belt (Sengör et al., 1999; Davis et al., 2001). The craton is divided into the Eastern Block, the Western Block and the intervening Trans-North China Orogen/Central Orogenic Belt (e.g., Zhao et al., 2005; Santosh, 2010; Kusky, 2011; Zhai and Santosh, 2011; Zhao and Zhai, 2013) (Fig. 1). The Eastern Block has experienced widespread tectonothermal reactivation since the Late Mesozoic, as manifested by the emplacement of voluminous Late Mesozoic mafic to felsic igneous rocks and Cenozoic basalts (e.g., Fan et al., 2000; Zhang et al., 2002, 2003; Gao et al., 2004; Zhang et al., 2004; Tang et al., 2006; Xu et al., 2006a, 2006b; Gao et al., 2008; W.L. Xu et al., 2008; Zhang et al., 2011).

The sample locations that we studied are shown in Fig. 1 and the major element compositions of these samples are summarized in the total alkalis–silica (TAS) diagram (Fig. 2). The ages of these basalts are shown in Table 1. The older basalts (>110 Ma) studied here were sampled from Liaoning and Shandong. Sihetun and Yixian basalts in western Liaoning are dated at 122–125 Ma (Zhou et al., 2003; Gao et al., 2008), while the Feixian basalts from western Shandong give a K–Ar age of 119 ± 2.3 Ma (Pei et al., 2004). The basalts are porphyritic with phenocrysts of olivine, clinopyroxene and minor orthopyroxene (Zhang et al., 2002; Pei et al., 2004; Gao et al., 2008). Olivine phenocrysts in the <110 Ma basalts have lower Fo (50–90) (Chi, 1987) compared with those in the >110 Ma basalts (mostly >90) (Pei et al., 2004; Gao et al., 2008). The major and trace element data of our studied samples have been previously published (Y.S. Liu et al., 2008 and references therein), except for samples 10HNB01, 10HNB02, and 10HNB03 from Hannuoba, Hebei Province, which are similar to those published in the literature. The samples in this study plot in basalt, picro-basalt, trachybasalt and tephrite fields on the TAS diagram (Fig. 2) with varying SiO_2 (39.70–50.52 wt.%). They are enriched in LREEs with low HREEs (Fig. 3), suggesting the presence of garnet as residual phase during mantle melting. In the primitive mantle normalized spidergram (Fig. 3), these basalts show compositional distinction. Samples of >110 Ma are characterized by relative Nb, Ta, and Ti depletion, resembling typical arc rocks (or the familiar "arc signature" or continental crustal signature) (e.g., Elliott, 2003; Rudnick and Gao, 2003). They also have relatively lower Nb/U and higher Sr/Y and Th/U ratios. On the other hand, samples of <110 Ma do not show Nb and Ta depletion, and actually resemble present-day OIB in many ways (Fig. 3). In addition, previous researches have suggested that the >110 Ma basalts have negative ε_{Nd}, variable $^{87}Sr/^{86}Sr_i$, unradiogenic Pb isotope ratios (e.g., Xu, 2001; Zhang et al., 2002, 2004; Gao et al., 2008), whereas the <110 Ma basalts with mantle-like Sr–Nd–Pb isotopes (e.g., Zhang and Zheng, 2003; Tang et al., 2006; Chen et al., 2009; J.J. Zhang et al., 2009; Wang et al., 2011). A recent study indicates that these two groups also have distinct Mg isotopic compositions (W. Yang et al., 2012). Here, we emphasize the new insights gained from Hf (combined with Sr, Nd) isotopes.

3. Analytical methods

Samples were trimmed to remove altered surfaces, crushed in a specially designed steel jaw crusher, and dried before powdered in a tungsten carbide mortar to a grain size <200 mesh for analysis. Major element compositions were analyzed by X-ray fluorescence (XRF; Rikagu RIX 2100) using fused glass disks at Northwest University, China following Rudnick et al. (2004). The samples for trace element analysis were digested using HF + HNO_3 in Teflon bombs and analyzed with an Agilent 7500a ICP-MS at Northwest University, China following Rudnick et al. (2004).

The Sr and Nd isotopic compositions were determined on MC-ICPMS (Nu Plasma HR, Nu Instruments, Wrexham, UK) in static mode at Northwest University, Xi'an. Approximately 100 mg whole-rock powders were digested in sealed Teflon bombs with a mixture of concentrated HNO_3, HF and $HClO_4$. The sealed bombs were kept in an oven at 190 °C for 48 h. The decomposed samples were then dried at 140 °C

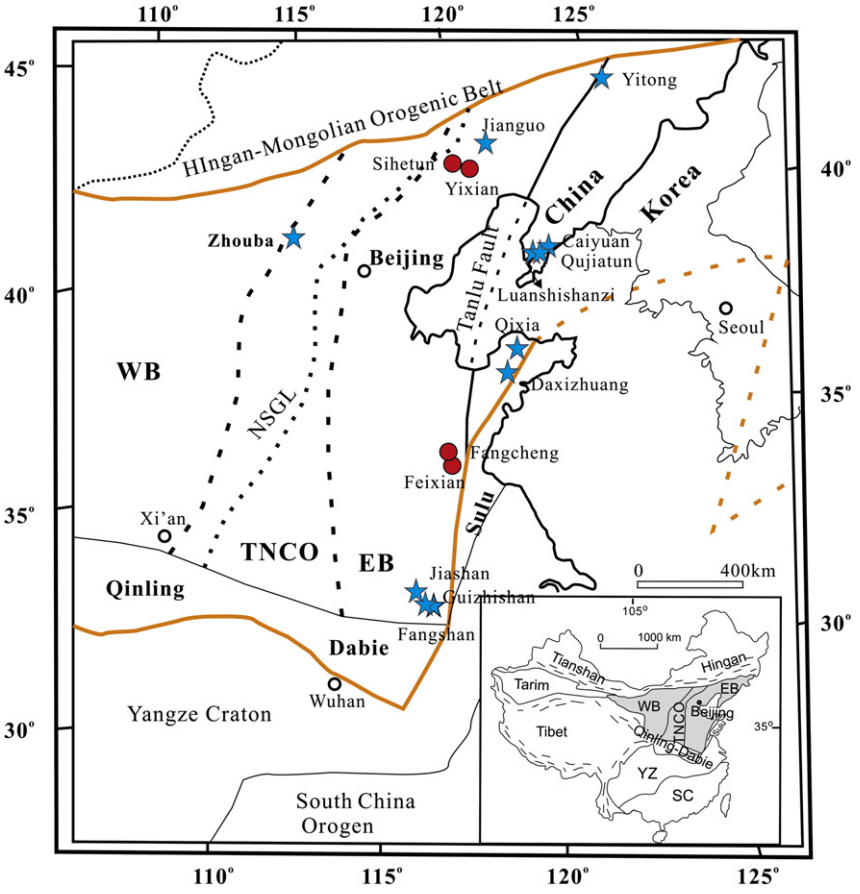

Fig. 1. Geologic sketch map of the North China Craton (NCC; after Gao et al., 2008). Red circles and blue stars represent samples of >110 Ma and <110 Ma, respectively. WB stands for the Western Block, TNCO for the Trans-North China Orogen and EB for the Eastern Block of the NCC (Zhao et al., 2005). The inset shows major tectonic divisions of China, where the North China Craton is shaded and YZ and SC denote the Yangtze Craton and South China Orogen, respectively.

followed by adding concentrated HNO_3 and HCl. Sr and Nd (and other REEs) were separated/concentrated using standard chromatographic columns with AG50W-X8 and HDEHP resins following the procedure of Gao et al. (2004). The measured $^{143}Nd/^{144}Nd$ and $^{87}Sr/^{86}Sr$ ratios were normalized to $^{146}Nd/^{144}Nd = 0.7219$ and $^{86}Sr/^{88}Sr = 0.1194$, respectively. External reproducibility of the isotopic measurements can

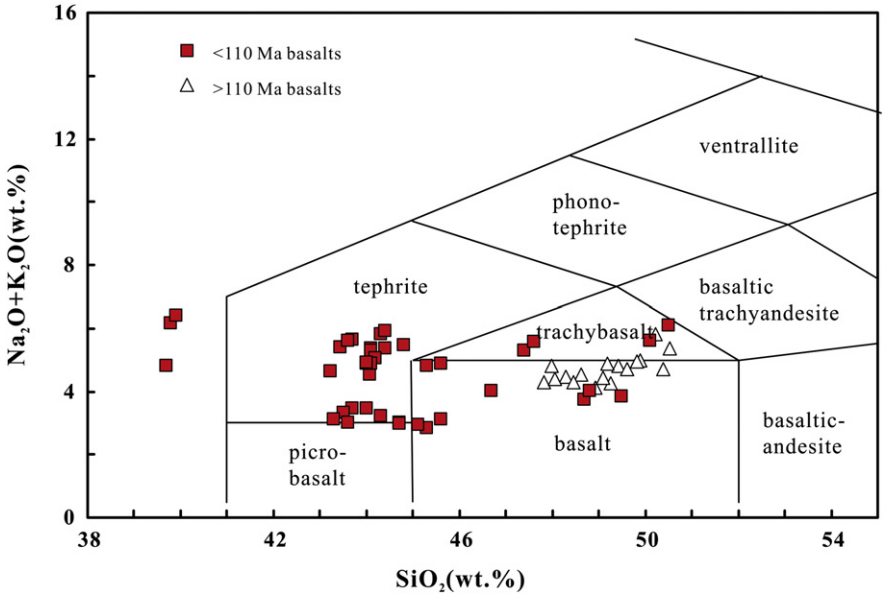

Fig. 2. Variations in $Na_2O + K_2O$ vs. SiO_2 (TAS, Le Maitre et al., 1989) for Mesozoic to Cenozoic basaltic samples from the North China Craton (NCC). Three samples from Qixia in Shandong Province have $SiO_2 < 40\%$, and are SiO_2 under-saturated olivine nephelinite.
Data are from Y.S. Liu et al. (2008).

Table 1
Sr–Nd–Hf isotopic compositions of Mesozoic to Cenozoic lavas from the North China Craton.

	Age	$^{147}Sm/^{144}Nd$	$^{143}Nd/^{144}Nd$		2σ	T_{DM} (Ma)	$\varepsilon_{Nd}(t)$	$^{87}Rb/^{86}Sr$	$^{87}Sr/^{86}Sr$		2σ	$^{87}Sr/^{86}Sr$ (t)	$^{176}Lu/^{177}Hf$	$^{176}Hf/^{177}Hf$		2σ	T_{DM} (Ma)	$\varepsilon_{Hf}(t)$
SHT-16	124–125 Ma; Gao et al. (2008)												0.008799	0.282633	±	59	1.1	−2.8
SHT-19													0.008813	0.282553	±	11	1.2	−5.7
SHT-21													0.008485	0.282544	±	28	1.2	−5.9
SHT-24													0.008121	0.282486	±	33	1.3	−8.0
SHT-31													0.008286	0.282562	±	51	1.2	−5.3
YX-25	122–125 Ma; Zhou et al. (2003)												0.009275	0.282332	±	16	1.7	−13.5
YX-26													0.009623	0.282265	±	36	1.8	−15.9
YX-26 dup													0.009623	0.282286	±	27	1.8	−15.2
YX-28													0.009612	0.282346	±	17	1.7	−13.0
YX-29													0.009020	0.282290	±	25	1.7	−15.0
YX-30													0.008898	0.282317	±	19	1.7	−14.0
SFC-05	124.9 Ma; Zhang et al. (2002)												0.006533	0.282198	±	72	1.7	−18.0
SFC-09													0.006469	0.282271	±	15	1.6	−15.4
SFC-17													0.006596	0.282272	±	48	1.6	−15.4
FX2-88	119 Ma; Pei et al. (2004)												0.006287	0.282352	±	83	1.5	−12.5
SFX-13													0.006316	0.282299	±	18	1.6	−14.4
SFX-27													0.006406	0.282216	±	23	1.7	−17.4
SFX-49													0.006267	0.282359	±	80	1.5	−12.3
YT-01	10.4 Ma; Liu et al. (1992)	0.138	0.512712	±	2	0.9	1.51	0.0816	0.705289	±	3	0.705277	0.005925	0.282941	±	4	0.5	6.2
YT-02		0.138	0.512741	±	2	0.8	2.09	0.0899	0.705319	±	4	0.705306	0.006687	0.282970	±	8	0.5	7.2
YT-53		0.122	0.512881	±	1	0.4	4.83	0.0940	0.703833	±	4	0.703820	0.007654	0.283039	±	3	0.4	9.6
JG-3	100.4 Ma; Zhang and Zheng (2003)												0.008564	0.282969	±	10	0.5	8.6
JG-4													0.008257	0.282963	±	7	0.5	8.4
JG-5													0.008579	0.282953	±	11	0.5	8.0
JG-6													0.008234	0.282968	±	9	0.5	8.6
JG-35													0.008688	0.282966	±	6	0.5	8.5
JG-37		0.124	0.512819	±	1	0.6	4.47	0.1842	0.703828	±	5	0.703566	0.008881	0.282981	±	7	0.5	9.0
JG-37 dup		0.124	0.512828	±	2	0.5	4.63	0.1842	0.703839	±	5	0.703577	0.008881	0.282989	±	12	0.5	9.3
10HNB-01	14.11–17.19 Ma; Wang et al. (1988)	0.126	0.512896	±	1	0.4	6.21	0.2097	0.723634	±	3	0.723247	0.003140	0.282989	±	3	0.4	8.0
10HNB-02		0.125	0.512884	±	1	0.5	5.98	0.1691	0.722421	±	4	0.722109	0.003560	0.282979	±	6	0.4	7.6
10HNB-02 dup		0.125	0.512882	±	2	0.5	5.95	0.1691	0.722242	±	20	0.721930						
10HNB-03		0.128	0.512879	±	2	0.5	5.84	0.0864	0.703983	±	4	0.703823	0.005828	0.282976	±	7	0.4	7.5
ZB-02	22.8 Ma; Liu et al. (1992)	0.127	0.512861	±	1	0.5	4.53	0.1141	0.704092	±	4	0.704060	0.004423	0.282932	±	25	0.5	6.1

(continued on next page)

Table 1 (*continued*)

	Age	$^{147}Sm/^{144}Nd$	$^{143}Nd/^{144}Nd$		2σ	T_{DM} (Ma)	$\varepsilon_{Nd}(t)$	$^{87}Rb/^{86}Sr$	$^{87}Sr/^{86}Sr$		2σ	$^{87}Sr/^{86}Sr$ (t)	$^{176}Lu/^{177}Hf$	$^{176}Hf/^{177}Hf$		2σ	T_{DM} (Ma)	$\varepsilon_{Hf}(t)$
ZB-10		0.146	0.512757	±	3	0.9	2.45	0.1337	0.704859	±	4	0.704821	0.006937	0.282947	±	8	0.5	6.5
ZB-12		0.145	0.512760	±	1	0.9	2.5	0.1317	0.704853	±	4	0.704816	0.008174	0.282921	±	49	0.6	5.6
ZB-15		0.141	0.512758	±	1	0.8	2.48	0.1275	0.704752	±	4	0.704716	0.007443	0.282960	±	8	0.5	7.0
WF1-1	36.3–39.3 Ma; Wang et al. (2007)												0.006062	0.282896	±	8	0.6	5.1
WF1-1 dup													0.006062	0.282909	±	14	0.6	5.6
WF1-2													0.005900	0.282879	±	12	0.6	4.5
WF2-1													0.005967	0.282969	±	13	0.5	7.7
WF2-2													0.005869	0.282948	±	8	0.5	6.9
WF2-4													0.006231	0.282962	±	18	0.5	7.4
WF2-7													0.006166	0.282926	±	17	0.5	6.2
WF2-7 dup													0.006166	0.282940	±	12	0.5	6.7
DD18-1	58.4 Ma; Wang et al. (2006)												0.006691	0.283032	±	31	0.4	10.2
DD18-4													0.006542	0.283040	±	16	0.4	10.5
DD18-4 dup													0.006542	0.283048	±	11	0.3	10.8
DD19-1	81.6 Ma; Wang et al. (2006)												0.005792	0.283027	±	12	0.4	10.5
DD19-2													0.005659	0.283011	±	13	0.4	9.9
DD19-3													0.005945	0.283033	±	11	0.4	10.7
QX-77	8.1–6.2 Ma; Liu et al. (1992)	0.112	0.512857	±	1	0.4	4.38	0.0462	0.703710	±	5	0.703703	0.003005	0.282978	±	9	0.4	7.5
QX-92		0.111	0.512850	±	2	0.4	4.25	0.0613	0.703848	±	6	0.703839						
QX-99		0.111	0.512845	±	1	0.5	4.14	0.0198	0.703706	±	4	0.703703	0.003013	0.282975	±	8	0.4	7.4
DX-6	73.0 Ma; Yan et al. (2005)	0.125	0.512886	±	2	0.5	5.48	0.1014	0.703636	±	4	0.703535	0.006011	0.283014	±	16	0.4	9.8
DX-9		0.126	0.512910	±	2	0.4	5.94	0.0929	0.703849	±	4	0.703757	0.006290	0.283034	±	7	0.4	10.5
DX-17		0.125	0.512885	±	1	0.5	5.47	0.1024	0.703630	±	4	0.703528	0.006279	0.283028	±	7	0.4	10.3
DX-23		0.126	0.512886	±	1	0.5	5.48	0.1011	0.704038	±	5	0.703937	0.006268	0.283021	±	34	0.4	10.0
FS00-55	8.6 Ma; Liu et al. (1992)	0.132	0.512957	±	2	0.4	6.3	0.1681	0.703539	±	5	0.703515	0.006110	0.283094	±	4	0.3	11.6
FS00-59		0.135	0.512931	±	2	0.4	5.79	0.1808	0.703465	±	5	0.703439	0.006229	0.283093	±	7	0.3	11.5
GZS00-01		0.124	0.512935	±	2	0.4	5.89	0.1029	0.703547	±	4	0.703532	0.006110	0.283049	±	8	0.3	10.0
GZS00-01 dup													0.006110	0.283055	±	5	0.3	10.2
GZS00-02		0.122	0.512926	±	1	0.4	5.71	0.0963	0.703587	±	5	0.703573	0.005638	0.283035	±	8	0.4	9.5
GZS00-08		0.127	0.512907	±	2	0.4	5.34	0.1259	0.703700	±	4	0.703682	0.006884	0.283031	±	6	0.4	9.3
LS99-01	1.41 Ma; Liu et al. (1992)	0.13	0.512811	±	1	0.6	3.37	0.0905	0.703756	±	4	0.703756	0.005808	0.282914	±	25	0.5	5.0
LS99-03		0.131	0.512884	±	2	0.5	4.81	0.0793	0.704152	±	4	0.704152	0.005691	0.282964	±	27	0.5	6.8

dup, duplicate analysis.

The Nd model age based on depleted mantle (DM) assumes a linear evolution of isotopic composition from $\varepsilon_{Nd}(T) = 0$ at 4.56 Ga to approximately +10 at the present time. Model ages (T_{DM}) were calculated using equations:

$T_{DM} = 1/\lambda \times \ln\{1 + [(^{143}Nd/^{144}Nd)_{sample} - 0.51315] / [(^{147}Sm/^{144}Nd)_{sample} - 0.2137]\}$, where the decay constant (λ) of ^{147}Sm used in model age calculation is 0.00654 Ga^{-1}.

$\varepsilon_{Nd}(t)$ was calculated using equation:

$\varepsilon_{Nd}(t) = 10000 \times [(^{143}Nd/^{144}Nd)_{sample} - (^{143}Nd/^{144}Nd)_{chondrite}] / (^{143}Nd/^{144}Nd)_{chondrite}$, where subscript sample and chondrite denote values of sample and chondrite at the time of sample formation.

The Hf model ages (T_{DM}) were calculated using equations:

$T_{DM} = 1/\lambda \times \ln\{1 + [(^{176Hf}/^{177}Hf)_{sample} - 0.28325] / [(^{176}Lu/^{177}Hf)_{sample} - 0.0384]\}$, where the decay constant (λ) of ^{176}Lu used in model age calculation is 0.01867 Ga^{-1}.

$\varepsilon_{Hf}(t)$ was calculated using equation:

$\varepsilon_{Hf}(t) = 10000 \times [(^{176}Hf/^{177}Hf)_{sample} - (^{176}Hf/^{177}Hf)_{chondrite}] / (^{176}Hf/^{177}Hf)_{chondrite}$, where subscript sample and chondrite denote values of sample and chondrite at the time of sample formation.

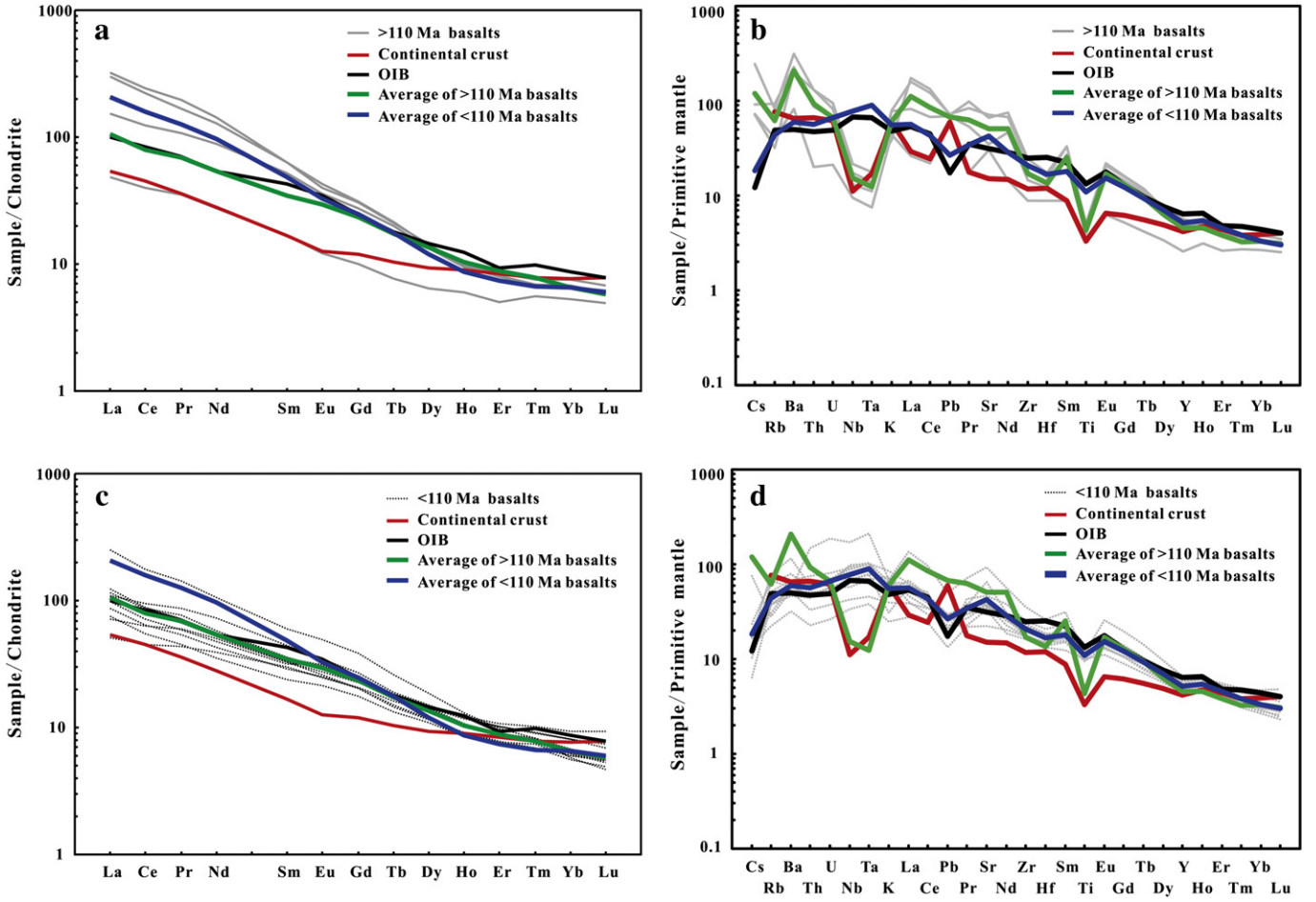

Fig. 3. (a, b) Chondrite normalized REE patterns and primitive mantle normalized trace-element patterns for older (>110 Ma) and (c, d) younger (<110 Ma) basaltic samples from the North China Craton. Chondrite values are from Taylor and McLennan (1985), and primitive mantle values from Sun and McDonough (1989). Continental crust and OIB values are from Rudnick and Gao (2003) and Sun and McDonough (1989), respectively.

be judged by repeated analyses of international standards. The La Jolla standard measured along with unknown samples gave an average $^{143}Nd/^{144}Nd$ of 0.511833 ± 0.000008 (2σ, n = 75), and NBS 987 gave $^{87}Sr/^{86}Sr$ =0.710233 ± 0.000035 (2σ, n = 28), which are identical to reference values within analytical errors. Analyses of BCR-2 gave $^{87}Sr/^{86}Sr$ =0.704995 ± 0.000039 (2σ, n = 3), and $^{143}Nd/^{144}Nd$ = 0.512611 ±0.000013 (2σ, n = 6).

The Hf isotopic analyses were done in static mode on the Nu Plasma MC-ICP-MS at Northwest University, Xi'an and Neptune Plus MC-ICP-MS at China University of Geosciences in Wuhan. About 300 mg of powders were digested in Teflon bombs with a mixture of concentrated HNO_3 + HF and dried on a hot plate. This was followed by addition of concentrated HNO_3, HF and $HClO_4$ sealed in bombs and kept in an oven at 190 °C. The samples were further digested by adding HNO_3, HCl and evaporation in sequence. Chromatographic column of LN-Spec resins was used for Hf separation and purification following Yuan et al. (2007). This method is modified after Münker et al. (2001), which reduces the time of separation and lowers the blank. The measured Hf isotopic ratios were corrected for isobaric interference with Lu at mass 176 by monitoring ^{175}Lu; the ^{176}Lu interference was subtracted by using a $^{176}Lu/^{175}Lu$ value of 37.69969 (Rosman and Taylor, 1997). During the course of our analysis, replicate measurements of the Hf standard JMC 475 gave 0.282179 ± 0.000019 (2σ, n = 16). Values reported for the samples are adjusted to the accepted value of 0.282160 for reference Hf standard JMC-475 (Vervoort and Blichert-Toft, 1999). Alfa Hf measured during the course of analysis gave an average $^{176}Hf/^{177}Hf$ of 0.282215 ± 0.000020 (2σ, n = 18), and BHVO-2 gave $^{176}Hf/^{177}Hf$ = 0.283090 ± 0.000036. BCR-2 and AGV-2 gave $^{176}Hf/^{177}Hf$ = 0.282872 ± 0.000023 and $^{176}Hf/^{177}Hf$ = 0.282983 ± 0.000014, respectively. All these are identical to their reference values within analytical errors.

4. Results

Analytical data of Sr–Nd–Hf isotopes are given in Table 1. Fig. 4 shows that the NCC basalts in Sr–Nd isotope space define a scattered negative trend. The >110 Ma samples are isotopically more enriched with low ε_{Nd} (t) (−1.69 to −14.93) and high $(^{87}Sr/^{86}Sr)_i$ (0.706137 to 0.709885), which is consistent with the previous reported Sr–Nd data (e.g. $\varepsilon_{Nd} < 0$) (e.g., Xu, 2001; Zhang et al., 2002; Gao et al., 2008; Yang and Li, 2008; Pei et al., 2011; D.B. Yang et al., 2012). The Feixian and Fangcheng basalts in western Shandong have more enriched Sr–Nd isotopic compositions than the Yixian basalts in western Liaoning. However, the Sr–Nd isotopic compositions for <110 Ma basaltic lavas are more depleted with low $(^{87}Sr/^{86}Sr)_i$ (0.703439 to 0.707545) and high ε_{Nd}(t) (+0.22 to +6.3), toward the depleted MORB mantle (DMM) (Fig. 4).

As for Hf isotopes, all the samples define a broad positive trend that is parallel to and lies within the terrestrial array (Fig. 5) in ε_{Hf} (t) vs. ε_{Nd} (t) diagram. The >110 Ma lavas display a large range of negative ε_{Hf}(t) (−18.0 to −2.8), consistent with an enriched source. In contrast, the <110 Ma lavas have more depleted Hf isotopic compositions with a smaller range of positive ε_{Hf}(t) (+4.5 to +11.6), which is consistent with the Sr–Nd isotopic characteristics. It is worth to note that although

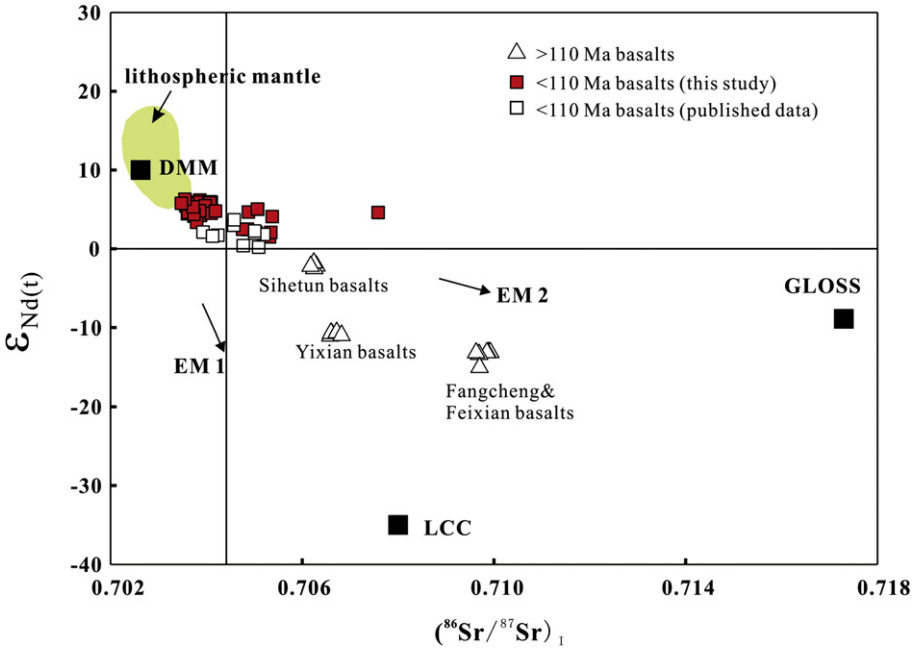

Fig. 4. Diagram of $\varepsilon_{Nd}(t)$ vs. initial $^{87}Sr/^{86}Sr$ showing Mesozoic to Cenozoic basaltic samples from the North China Craton, where (t) refers to the basalt eruption ages. Data for >110 Ma basalts are from Zhang et al. (2002), Gao et al. (2004) and Gao et al. (2008), and for <110 Ma basalts are from Zhang and Zheng (2003), Wang et al. (2006) and Wang et al. (2007). Data for LCC (model lower continental crust), GLOSS (Global subducting sediments) and DMM are from Jahn et al. (1999), Plank and Langmuir (1998) and Workman and Hart (2005), respectively. The trends for EM-I and EM-II are from Zindler and Hart (1986). The fields of lithospheric mantle are represented by peridotite xenoliths from Cenozoic basalts in Shanwang (Chu et al., 2009) and Beiyan (Xiao et al., 2010).

all the samples plot along the terrestrial array (Fig. 5), they do display some scattering; some samples show obvious deviation from the array most likely resulting from mantle source heterogeneity on varying local scales because these samples are from a geographically large area (see blue stars in Fig. 1). The effect of the asthenospheric heterogeneity on $\varepsilon_{Hf}(t)$ isotopes of the erupted basalts is most likely inherited from varying Lu/Hf ratios in the source regions.

5. Discussion

5.1. Petrogenesis of Mesozoic–Cenozoic basaltic rocks in the NCC

In contrast to oceanic basalts, continental basalts would pass through the thick continental crust prior to eruption. Thus, the effect of crustal contamination might be considered in their petrogenesis.

The occurrence of mantle xenoliths within these lavas suggests that they ascended rapidly, thus avoiding significant interaction with crust and wall-rock. The OIB-like features of the <110 Ma basalts (e.g., high Ce/Pb, high Nb/U, and low La/Nb ratios) further ruled out the significant crustal contamination. In addition, the majority of the <110 Ma basalts have MgO > 8 wt.% and the >110 Ma basalts have even higher MgO, which rule out significant crustal contamination. Therefore, there was no significant interaction between the basaltic magmas and the continental crust during magma ascent.

The data and foregoing discussion demonstrate that the NCC basalts show compositional distinction between older basalts (>110 Ma) and younger ones (<110 Ma). This time-dependent difference or division points to their contrasting differences in their sources or processes or both.

The >110 Ma basalts are isotopically enriched with $\varepsilon_{Nd} < 0$ and $\varepsilon_{Hf} < 0$. They all fall along the terrestrial array (Fig. 5). The Hf isotopes in this study are consistent with the Hf data of Fangcheng basalts reported by Yang et al. (2006). Previous studies indicate that the Mesozoic basalts derived from an isotopically enriched mantle source with negative ε_{Nd}, variable $^{87}Sr/^{86}Sr_i$, unradiogenic Pb isotope ratios (e.g., Xu, 2001; Zhang et al., 2002; Gao et al., 2008; Yang and Li, 2008). In addition, the >110 Ma basalts have significant Nb, Ta, and Ti depletion (also see Fig. 3) and high Nb/Ta ratios, and Nb and Ta are both negatively correlated with MgO, which can be interpreted as indicating a low Nb and Ta mantle source with high Nb/Ta ratios (Y.S. Liu et al., 2008). Compared with rocks from mantle derived magmas in all geological environments, Nb–Ta–Ti depletion is characteristic of volcanic arc rocks or the "arc-signature" shared by continental crustal materials. Combined with their relatively low Nb/U, high Sr/Y and Th/U ratios, it has been interpreted that the >110 Ma basalts may have continental crust involved in their petrogenesis (e.g., Zhang et al., 2002; Gao et al., 2008; W.L. Xu et al., 2008; Y.S. Liu et al., 2008; Yang and Li, 2008; Xu et al., 2010) (Fig. 6). Our new Hf data cannot rule out any continental crustal contribution, there are still some questions to be resolved. The Nb–Ta–Ti depletion could be interpreted as the presence of rutile as a residual phase, but this would require the source rock to be basaltic (e.g., eclogite). However, partial melting of eclogites cannot produce basaltic melts (see Fig. 2) we studied here, and importantly, rutile has very high solubility in silicate melt and cannot exist as a residual phase during basalt melting (Ryerson and Watson, 1987). Basaltic melts must be produced by partial melting of mantle peridotites or pyroxenites formed via interaction of peridotite with melt from eclogite (references in Gao et al., 2008). The contribution of recycled continental crust with imparted Nb–Ta–Ti signature could be invoked, but the amount of such crustal material required to explain the strong Nb–Ta–Ti signature needs further investigation to see if it would be too large and would produce much more felsic melt rather than basalts.

Alternatively, metasomatism might explain the large negative ε_{Nd} and ε_{Hf} values of the >110 Ma basalts. While sub-continental mantle lithosphere as a result of previous melt extraction is likely depleted in major elements (i.e., high $Mg^{\#}$, low Al_2O_3 and high CaO/Al_2O_3), it can be enriched in terms of incompatible elements throughout its long histories through mantle metasomatism (e.g., O'Reilly and Griffin, 1988), in processes similar to that taking place at the lithosphere–asthenosphere boundary beneath ocean basins (Niu and O'Hara, 2003, 2009) or in a mantle wedge environment (Donnelly et al., 2004). The metasomatism would not significantly affect the major elements, but will result in the

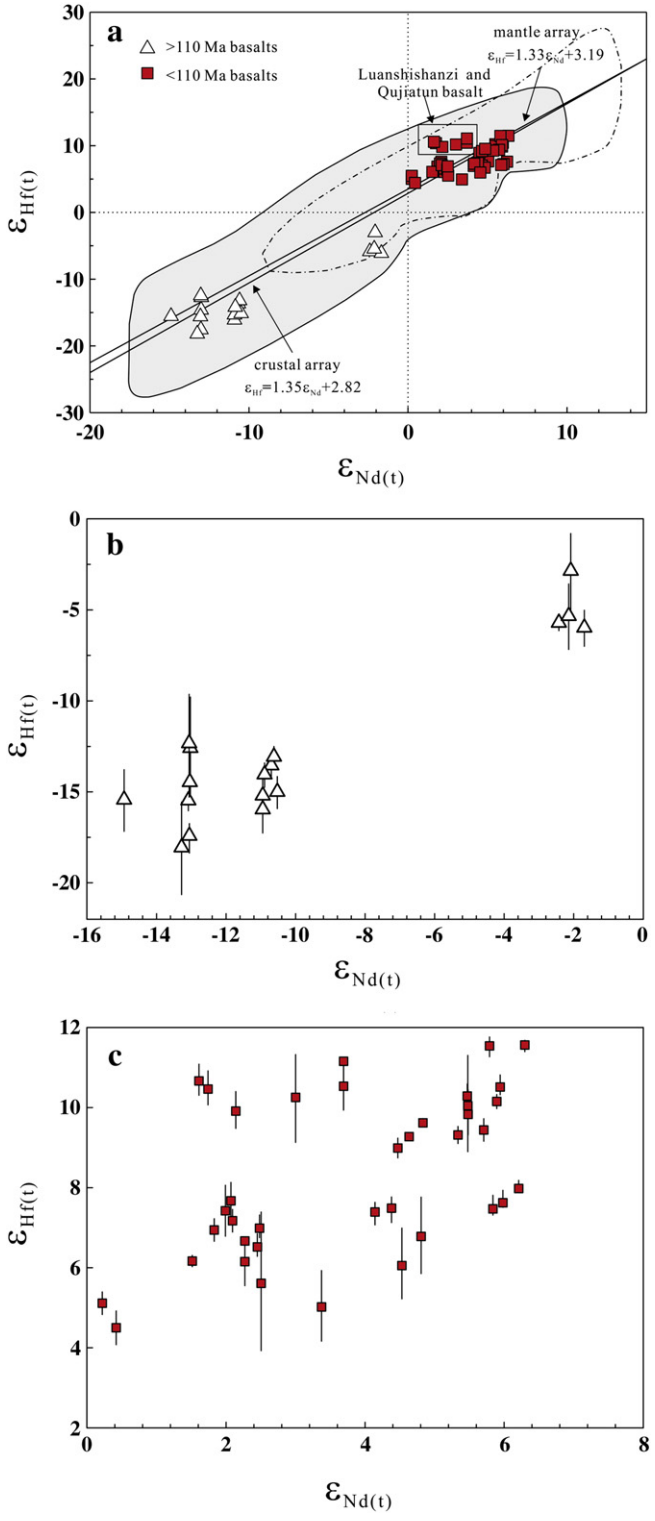

Fig. 5. (a) Diagram of ε_{Hf} vs. ε_{Nd} showing Mesozoic to Cenozoic basaltic rocks from the North China Craton. The field for Hf–Nd crust–mantle array is from Vervoort et al. (1999). (b) Close-up of portion of (a) to illustrate the 2σ analytical error bar of ε_{Hf} for >110 Ma basalts. (c) Close-up to illustrate the 2σ analytical error bar of ε_{Hf} for <110 Ma basalts. The 2σ analytical error for most of these basalts is within ±1 epsilon unit, although several >110 Ma basalts have a large error of ~3 epsilon units as shown.

enrichments of volatiles and progressively more incompatible elements, e.g., the elevated ratios of Rb/Sr, Nd/Sm and Hf/Lu, which can also explain the isotopically enriched signatures in the >110 Ma basalts (i.e., high $^{87}Sr/^{86}Sr$, low $\varepsilon_{Nd}[t]$ and $\varepsilon_{Hf}[t]$).

The mantle lithosphere, by definition, is too cold to melt and is not the dominant source of basaltic magmas, but it can participate in basaltic magmatism if there is thermal perturbation, which would not affect the bulk lithosphere, but can readily melt its metasomatic components because of their low solidus temperatures (Niu, 2005, 2008). The thermal perturbation could be related to the lithosphere thinning in the Mesozoic without the need of mantle plumes which did not exist in eastern China at least since the Mesozoic (see Niu, 2005) because of the presence of the cold Pacific plate in the mantle transition zone (Kárason and van der Hilst, 2000; Zhao et al., 2004) that prevents hot deep plumes to rise from below and to develop above (Niu, 2005).

The stagnant Pacific plate in the transition zone will inevitably undergo isobaric heating, which will result in phase changes from water-rich to water-poor, and to anhydrous minerals. This transition-zone dehydration process will facilitate the production of hydrous melt that ascends and migrates upwards to weaken the base of the ancient lithosphere by hydration, i.e., basal hydration weakening, which can effectively convert the basal lithospheric mantle into the asthenospheric mantle. This is in effect the process of lithosphere thinning (Niu, 2005), accompanied by the surface volcanism with the ascending hydrous melt assimilated with the metasomatic components in the prior lithosphere to form geochemically enriched basaltic melts (Niu, 2005), i.e., the >110 Ma basaltic melts in the NCC (Fig. 6).

It should be noted that the effect of transition-zone slab dehydration differs from subduction-zone metamorphic dehydration in triggering arc magmatism and arc rocks characterized by enrichments of water-soluble elements but depleted in water-insoluble high field strength elements (e.g., Nb, Ta and Ti). The transition-zone dehydration is a magmatic process producing hydrous melt that rises and weakens the base of the lithosphere (Niu, 2005). Such hydrous melt should be compositionally characterized by, and more enriched than, OIB. However, the >110 Ma basaltic melt resulted from hydration-weakened lithosphere with inherited composition (i.e., depletion in Nb, Ta and Ti) of prior metasomatic origin (Niu, 2005).

The above two models both can explain the "arc signatures" and enriched isotopic compositions. Unfortunately, our new data could not give more constrains on these. Hf data are consistent with Nd isotopes.

The <110 Ma basaltic rocks are isotopically depleted with low $^{87}Sr/^{86}Sr_i$, $\varepsilon_{Nd} > 0$ and $\varepsilon_{Hf} > 0$, which is consistent with the previously reported Sr–Nd–Pb–Hf data (e.g., Zou et al., 2000; Zhang and Zheng, 2003; Xu et al., 2005; Tang et al., 2006; Yang et al., 2006; Yang and Li, 2008; Chen et al., 2009; Zeng et al., 2011). In terms of trace elements, all the <110 Ma basaltic rocks are enriched in incompatible elements and decoupled with the depleted isotopic compositions. The "garnet signatures" (i.e., $[Sm/Yb]_N > 1$) suggest that melting should happen at the garnet peridotite stability field. These younger samples resemble present-day OIB in many ways without Nb and Ta depletion and slightly negative Pb anomalies (Fig. 3).

Various hypotheses have been put forward to explain these characteristic features. Many previous studies inferred a convective asthenospheric source (e.g., Zou et al., 2000; Zhang and Zheng, 2003; Niu, 2005; Yang and Li, 2008). On the other hand, partial melting of the juvenile SCLM (pyroxenite formed by interaction between oceanic crustal-derived melt and overlying mantle-wedge peridotite) has also been proposed (J.J. Zhang et al., 2009; Wang et al., 2011). In addition, the recycled lower continental crust (e.g., Y.S. Liu et al., 2008; Chen et al., 2009; Zeng et al., 2011) and sub-continental lithospheric mantle (Xu et al., 2005; Tang et al., 2006) have been suggested to be involved in the mantle source.

Previous studies suggest that dewatering as well as melting of oceanic crust during subduction produce negative $\Delta\varepsilon_{Hf}$, which describes the deviation of a sample from the OIB array in the y-axis direction (e.g., Gaffney et al., 2007). However, our new Hf and Nd isotopes of <110 Ma basalts all plot along the terrestrial array. In addition, if the subducted oceanic crusts melt in the deep lower mantle, this melt, depending upon its composition, may have greater (up to 15%) density

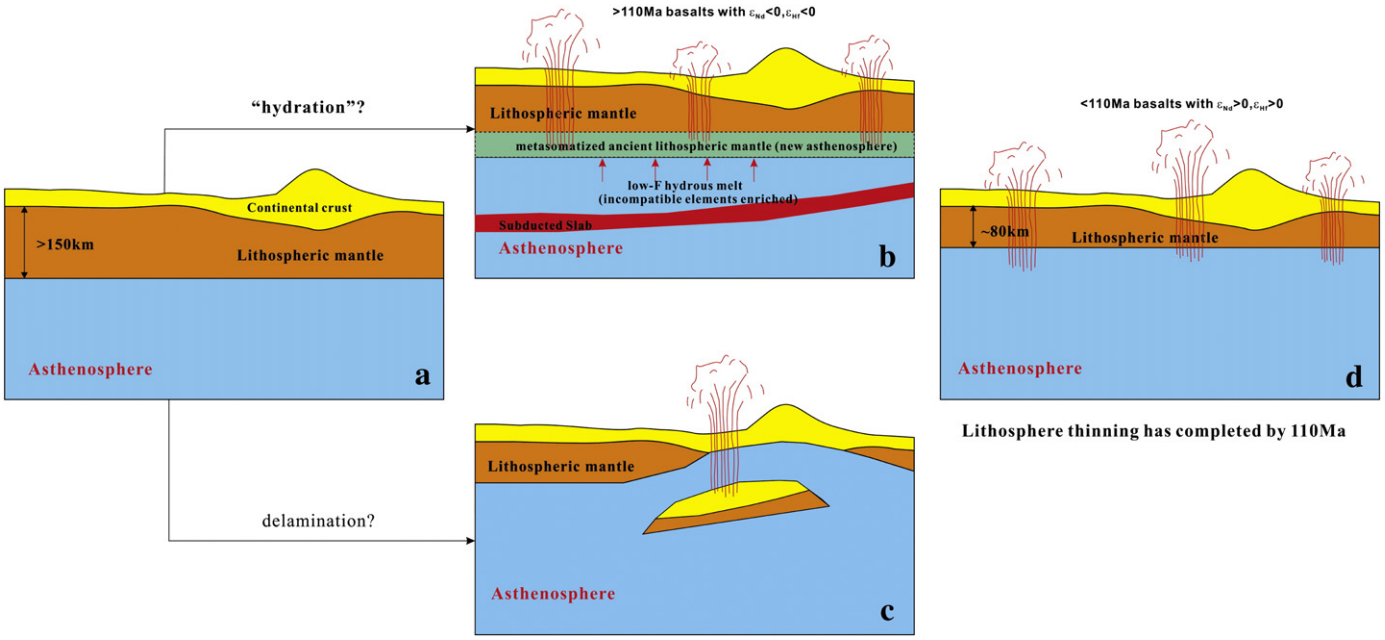

Fig. 6. Cartoon showing the possible petrogenesis of basaltic lavas from the North China Craton. The lithospheric mantle beneath the North China Craton is thick in the Paleozoic (a). The subducted slab (for illustration, but it is actually located in the mantle transition zone depth) dehydration process will weaken the base of the ancient lithosphere by hydration, which can effectively convert the basal lithospheric mantle into the "asthenospheric mantle". This is in effect the process of lithosphere thinning (Niu, 2005), accompanied by the geochemically enriched basaltic melts, i.e., the >110 Ma basaltic melts in the NCC (b). The >110 Ma lavas might also contain contributions from ancient continental crust in the process of lithosphere thinning as proposed by Gao et al. (2004) (c). The thinning of the lithosphere beneath the North China Craton must have been completed by ~110 Ma. The <110 Ma lavas were most likely derived from the asthenosphere when the lithosphere had already been thinned (d).

than solid peridotitic mantle (Niu and O'Hara, 2003). Therefore, it is difficult to ascend. These basalts might not derive from the juvenile SCLM formed by interaction between oceanic crustal-derived melt and overlying mantle-wedge peridotite.

Previous studies of Cenozoic basalts in the NCC have suggested an asthenospheric source with the contributions of subcontinental lithospheric mantle as the enriched end-member (Xu et al., 2005; Tang et al., 2006). Recycled lithospheric mantle has a variably higher $^{176}Hf/^{177}Hf$ at a given $^{143}Nd/^{144}Nd$ as has been observed in Hawaiian peridotite xenoliths and abyssal peridotites in oceanic settings (Bizimis et al., 2004; Stracke and Snow, 2009) and peridotite xenoliths from continents (Chu et al., 2009; Xiao et al., 2010). The coupled Hf and Nd isotopes of <110 Ma basalts indicate that the contributions of subcontinental lithospheric mantle are insignificant.

The recycled lower continental crust has also been suggested to be the enriched end-member in depleted asthenospheric mantle source of <110 Ma basalts (Y.S. Liu et al., 2008; Chen et al., 2009; Zeng et al., 2011). The melting of recycled eclogites will increase their $^{176}Lu/^{177}Hf$ ratios more strongly than $^{147}Sm/^{144}Nd$ ratios, because the HREEs are compatible in garnet (e.g., van Westrenen et al., 1999). Thus, the residue will evolve in time toward highly radiogenic Hf isotopes but more moderately radiogenic Nd isotopes. It seems apparent that re-melting of this residue would produce the decoupled Hf and Nd isotopes as interpreted by Chen et al. (2009) and Zeng et al. (2011). However, if the eclogites are residues of subduction dehydration metamorphism (not melting residues), the bulk-rock Lu/Hf should be unchanged, and melting of such eclogites should not produce melt with decoupled Nd–Hf isotopes. Hence, the interpretation in the literature may not be valid. Importantly, the <110 Ma basalts except those from Luanshishanzi and Qujiatun have coupled Hf and Nd isotopes, which might not support significant involvement of recycled lower continental crust in mantle source of <110 Ma basalts.

The straightforward interpretation for the petrogenesis of the <110 Ma basalts with more depleted Sr–Nd–Hf isotopic composition is that the sources are normal fertile asthenosphere after the cratonic lithospheric root had been removed prior to 110 Ma (Fig. 6). Zhang and Zheng (2003) indicate that the Jianguo basalts (100.4 Ma) show asthenospheric isotope signature, thus the lithosphere beneath this region could be no more than 65 km. Since ~110 Ma, the asthenospheric melting began in the garnet peridotite stability field, but may undergo greater extent of melting because of the already thinned lithosphere that allowed decompression melting continued to a shallow level (Niu et al., 2011).

The question remains why decompression melting could have taken place. One possibility is the western Pacific subduction-induced asthenospheric flow from beneath the thickened lithosphere in the west towards beneath the thinned lithosphere to the east, where decompression can take place and explain the Cenozoic basaltic magmatism in the NCC as well as the geochemical characteristics (Niu, 2005). The extension induced by the western Pacific subduction might further facilitate lithosphere thinning in eastern China. In this context, we should note the apparent isotope-trace element decoupling in the <110 Ma basalts. That is, the association of the depleted isotopes (e.g., relatively low $^{87}Sr/^{86}Sr$, and high–low $\varepsilon_{Nd}[t]$ and $\varepsilon_{Hf}[t]$) with enriched incompatible elements (e.g., $[La/Sm]_N \gg 1$ and $[Sm/Yb]_N \gg 1$; see Fig. 3). This is in fact a global phenomenon, and is actually associated with a straightforward process as a result of recent or even current enrichment process that is too short to produce enough radiogenic ingrowths for isotopes (see Niu et al., 1996). The paleo-pacific plate still exists today in the mantle transition zones beneath eastern China, and its dehydration, hydrous melt formation (enriched in volatiles and incompatible elements) and its percolation through the upper mantle during ascent continues to refertilize the melting asthenosphere, giving rise to the incompatible elements enriched and isotopically depleted younger (<110 Ma) basalts. Previous studies have attributed this decoupling to metasomatism by SiO_2-rich melt derived from subducted oceanic crust of the western Pacific plate (Yang and Li, 2008). A recent study found that the <110 Ma basalts exhibit light Mg isotopic composition, and the source might be metasomatized by carbonate melt from the subducted Pacific oceanic crust (W. Yang et al., 2012). Bizimis et al. (2003) showed that mantle carbonate assemblages are capable of producing anomalously radiogenic Hf on a short timescale (10–50 Myr)

due to their extremely high Lu/Hf, while leaving the Nd isotopes unaffected. Hence, melting of aged mantle carbonate would result in a significant departure from the terrestrial Nd–Hf isotope array along a vertical trend. While this is an important contribution, this proposed scenario is inconsistent with the Hf–Nd data in this study. Future studies are required to test the contribution of the carbonate melt. In any case, the subducted Pacific plate may play an important role in generating the <110 Ma basalts.

5.2. The significance of Hf–Nd isotopes

The Hf–Nd isotopic data of <110 Ma basalts show a scattered trend parallel to and within the terrestrial array defined by crustal and mantle rocks (Vervoort et al., 1999) with some obvious deviation (Fig. 5). Some samples plot below the mantle array, while others above the array. However, they all plot within the array and have similar Hf and Nd isotopic compositions for each area. The deviation and scatter beyond the analytical errors are likely reflecting source heterogeneity genetically related to sources and histories (i.e., varying Lu/Hf ratios most likely controlled by modal variation of garnet as a residual phase during previous melt extraction) on varying local scales because these samples are from a geographically large area. However, basalts from Luanshishanzi and Qujiatun close to each other in geography have shallower slope. Their slightly higher $^{176}Hf/^{177}Hf$ ratios at given Nd isotopic compositions (Fig. 5) could reflect mantle sources containing components of pelagic sediments (Chauvel and Blichert-Toft, 2001; Bertrand et al., 2003; Doucet et al., 2004; Janney et al., 2005; Salters et al., 2006) or lower crustal mafic material (Vervoort et al., 2000; Schmitz et al., 2004; Y.S. Liu et al., 2008; Chen et al., 2009; Zeng et al., 2011), but recycled lithospheric mantle may be a much better candidate as variably higher $^{176}Hf/^{177}Hf$ at a given $^{143}Nd/^{144}Nd$ has been observed in Hawaiian peridotite xenoliths and abyssal peridotites in oceanic settings (Bizimis et al., 2004; Stracke and Snow, 2009) and peridotite xenoliths from continents (Chu et al., 2009; Xiao et al., 2010). In this context, it is probable that recycled ancient metasomatized deep portions of mantle lithosphere, both continental (McKenzie and O'Nions, 1995) and oceanic (Niu and O'Hara, 2003), are important material for incompatible element enriched OIB and some continental basalts, including <110 Ma basalts from the NCC that we study here.

6. Conclusions

A whole-rock Hf isotope study of Mesozoic–Cenozoic basalts from the NCC has offered new perspectives on the petrogenesis of these rocks in the context of mantle evolution in eastern China. These include:

1) The older >110 Ma basalts and younger <110 Ma basalts are distinctively different in both Hf–Nd isotopes and incompatible element systematics. The >110 Ma basalts have enriched Hf–Nd isotopic compositions with arc-like trace element signatures (i.e., relatively depleted in HFSEs). By contrast, the <110 Ma basalts have more depleted Hf–Nd isotopic compositions with present-day OIB-like trace element patterns. This confirms previous documentation using Sr–Nd isotopes and trace elements.
2) The petrogenesis of the >110 Ma basalts is most consistent with the mantle source with significant contributions from ancient metasomatized lithospheric mantle or continental crust. The magmatism represented by these basalts is coeval and genetically associated with the lithosphere thinning beneath the NCC. The petrogenesis of the <110 Ma basalts is most consistent with melting of asthenospheric mantle.
3) The compositional contrast between basalts erupted before and after ~110 Ma clearly indicates that the lithosphere thinning beneath the NCC indeed took place in the Mesozoic. Importantly and explicitly, the thinning of this ancient cratonic lithosphere had mainly ended by 110 Ma.
4) The geochemically enriched signatures of the metasomatized mantle lithosphere as reflected by the >110 Ma basalts suggest that such material, when transported into the asthenosphere through lithosphere thinning, may contribute to the geochemically enriched component for intra-plate volcanism like ocean island basalts and continental alkaline basalts.

Acknowledgments

H. L. Yuan, L. Zhou, C. L. Zong, M. N. Dai, H. H. Chen and J. Q. Wang are thanked for their help during the chemical separation and analyses. This study is supported by the National Nature Science Foundation of China (Grants 41273013, 41173016 and 90914007), the Specialized Research Fund for the Doctoral Program of Higher Education of China (20120211120034), and the Fundamental Research Funds for the Central Universities.

References

Bertrand, H., Chazot, G., Blichert-Toft, J., Thoral, S., 2003. Implications of widespread high-μ volcanism on the Arabian Plate for Afar mantle plume and lithosphere composition. Chemical Geology 198, 47–61.
Bizimis, M., Salters, V.J.M., Dawson, J.B., 2003. The brevity of carbonatite sources in the mantle: evidence from Hf isotopes. Contributions to Mineralogy and Petrology 145, 281–300.
Bizimis, M., Lassiter, J.C., Salters, V.J.M., Sen, G., Griselin, M., 2004. Extreme Hf–Os isotope compositions in Hawaiian peridotite xenoliths: Evidence for an ancient recycled lithosphere. Eos Transations AGU 85 (47) (Fall Meet. Supplement, V51B-0550).
Chauvel, C., Blichert-Toft, J., 2001. A hafnium isotope and trace element perspective on melting of the depleted mantle. Earth and Planetary Science Letters 190, 137–151.
Chen, L.H., Zeng, G., Jiang, S.Y., Hofmann, A.W., Xu, X.S., Pan, M.B., 2009. Sources of Anfengshan basalts: subducted lower crust in the Sulu UHP belt, China. Earth and Planetary Science Letters 286, 426–435.
Chi, J.S., 1987. The Study of Cenozoic Basalts and the Upper Mantle Beneath Eastern China (Attachment: Kimberlite). China University of Geosciences Press, Beijing.
Chu, Z.Y., Wu, F.Y., Walker, R.J., 2009. Temporal evolution of the lithospheric mantle beneath the eastern North China Craton. Journal of Petrology 50, 1857–1898.
Davis, G.A., Zheng, Y.D., Wang, C., Darby, B.J., Zhang, C.H., Gehrels, G., 2001. Mesozoic tectonic evolution of the Yanshan fold and thrust belt, with emphasis on Hebei and Liaoning provinces, northern China. In: Hendrix, H.S., Davis, G.A. (Eds.), Paleozoic and Mesozoic Tectonic Evolution of Central Asia: From Continental Assembly to Intracontinental Deformation. Geological Society of America Memoir, 194, pp. 171–197.
Deng, J.F., Mo, X.X., Zhao, H.L., Luo, Z.H., Du, Y.S., 1994. Lithosphere root/de-rooting and activation of the East China continent. Geosciences 8, 349–356.
Deng, J.F., Zhao, H.L., Mo, X.X., Wu, Z., Luo, Z.H., 1996. Continental Root-Mantle Tectonics in China: A Key to Continental Dynamics. Geological Publishing House, Beijing 1–96.
Deng, J.F., Mo, X.X., Zhao, H.L., Wu, Z.X., Luo, Z.H., Su, S.G., 2004. A new model for the dynamic evolution of Chinese lithosphere: continental roots-plume tectonics. Earth Science Reviews 65, 223–275.
Deng, J.F., Su, S.G., Niu, Y.L., Liu, C., Zhao, G.C., Zhao, X.G., Zhou, S., Wu, Z.X., 2007. A possible model for the lithospheric thinning of North China Craton: evidence from the Yanshanian (Jura-Cretaceous) magmatism and tectonic deformation. Lithos 96, 22–35.
Donnelly, K.E., Goldstein, S.L., Langmuir, C.H., Spiegelman, M., 2004. Origin of enriched ocean ridge basalts and implications for mantle dynamics. Earth and Planetary Science Letters 226, 347–366.
Doucet, S., Weis, D., Scoates, J.S., Debaille, V., Giret, A., 2004. Geochemical and Hf–Pb–Sr–Nd isotopic constraints on the origin of the Amsterdam-St. Paul (Indian Ocean) hotspot basalts. Earth and Planetary Science Letters 218, 179–195.
Elliott, T., 2003. Tracers of the slab. Geophysical Monograph 138, 23–45.
Fan, W.M., Zhang, H.F., Baker, J., Jarvis, K.E., Mason, P.R.D., Menzies, M.A., 2000. On and off the North China Craton: where is the Archean keel? Journal of Petrology 41, 933–950.
Gaffney, A.M., Blichert-Toft, J., Nelson, B.K., Bizzarro, M., Rosing, M., Albarède, F., 2007. Constraints on source-forming processes of West Greenland kimberlites inferred from Hf–Nd isotope systematics. Geochimica et Cosmochimica Acta 71, 2820–2836.
Gao, S., Rudnick, R.L., Carlson, R.W., McDonough, W.F., Liu, Y.S., 2002. Re–Os evidence for replacement of ancient mantle lithosphere beneath the North China Craton. Earth and Planetary Science Letters 198, 307–322.
Gao, S., Rudnick, R.L., Yuan, H.L., Liu, X.M., Liu, Y.S., Xu, W.L., Ling, W.L., Ayers, J., Wang, X.C., Wang, Q.H., 2004. Recycling lower continental crust in the North China Craton. Nature 432, 892–897.
Gao, S., Rudnick, R.L., Xu, W.L., Yuan, H.L., Liu, Y.S., Walker, R.J., Puchtel, I.S., Liu, X.M., Huang, H., Wang, X.R., Yang, J., 2008. Recycling deep cratonic lithosphere and generation of intraplate magmatism in the North China Craton. Earth and Planetary Science Letters 270, 41–53.
Griffin, W.L., Zhang, A.D., O'Reilly, S.Y., Ryan, C.G., 1998. Phanerozoic evolution of the lithosphere beneath the Sino-Korean Craton. In: Flower, M.F.J., Chung, S.L., Lo, C.H., Lee, T.Y. (Eds.), Mantle Dynamics and Plate Interactions in East Asia. American Geophysical Union, Washington D. C., pp. 107–126.

Griffin, W.L., Pearson, N.J., Belousova, E., 2000. The Hf isotope composition of cratonic mantle: LAM-MC-ICPMS analysis of zircon megacrysts in kimberlites. Geochimica et Cosmochimica Acta 64, 133–147.
Huang, F., Li, S., Dong, F., Li, Q., Chen, F., Wang, Y., Yang, W., 2007. Recycling of deeply subducted continental crust in the Dabie Mountains, central China. Lithos 96, 151–169.
Jahn, B.M., Wu, F.Y., Lo, C.H., Tsai, C.H., 1999. Crust–mantle interaction induced by deep subduction of the continental crust: geochemical and Sr–Nd isotopic evidence from post-collisional mafic–ultramafic intrusions of the northern Dabie complex, central China. Chemical Geology 157, 119–146.
Janney, P.E., Le Roex, A.P., Carlson, R.W., 2005. Hafnium isotope and trace element constraints on the nature of mantle heterogeneity beneath the central southwest Indian ridge (13°E to 47°E). Journal of Petrology 46, 2427–2464.
Johnson, C.M., Shirey, S.B., Barovich, K.M., 1996. New approaches to crustal evolution studies and the origin of granitic rocks: what can the Lu–Hf and Re–Os isotope systems tell us? Royal Society of Edinburgh Transactions, Earth Sciences 87, 339–352.
Kárason, H., van der Hilst, R., 2000. Constraints on mantle convection from seismic tomography. Geophysical Monograph 121, 277–288.
Kusky, T.M., 2011. Geophysical and geological tests of tectonic models of the North China Craton. Gondwana Research 20, 26–35.
Le Maitre, R.W., Bateman, P., Dubek, A., Keller, J., Lameyre, J., Le Bas, M.J., Sabine, P.A., Schimid, R., Sorensen, H., 1989. A Classification of Igneous Rocks and Glossary of Terms: Recommendations of the International Union of Geological Sciences Subcommission the Systematics of Igneous Rocks. Blackwell Scientific Publication, Oxford.
Li, S.G., Xiao, Y., Liou, D., Chen, Y., Ge, N., Zhang, Z., Sun, S.S., Cong, B., Zhang, R., Hart, S.R., Wang, S., 1993. Collision of the North China and Yangtze Blocks and formation of coesite-bearing eclogites: timing and processes. Chemical Geology 109, 89–111.
Ling, W.L., Duan, R.C., Xie, X.J., Zhang, Y.Q., Zhang, J.B., Cheng, J.P., Liu, X.M., Yang, H.M., 2009. Contrasting geochemistry of the Cretaceous volcanic suites in Shandong province and its implications for the Mesozoic lower crust delamination in the eastern North China Craton. Lithos 113, 640–658.
Liu, D.Y., Nutman, A.P., Compston, W., Wu, J.S., Shen, Q.H., 1992. Remnants of >3800 Ma crust in the Chinese part of the Sino-Korean craton. Geology 20, 339–342.
Liu, D.Y., Wan, Y.S., Wu, J.S., Wilde, S.A., Zhou, H.Y., Dong, C.Y., Yin, X.Y., 2007. Eoarchean Rocks and Zircons in the North China Craton. In: van Kranendonk, M., Smithies, R.H., Bennett, V. (Eds.), Earth's Oldest Rocks, 15. Elsevier Series' Developments in Precambrian Geology, Amsterdam, The Netherlands, pp. 251–273.
Liu, D.Y., Wilde, S.A., Wan, Y.S., Wu, J.S., Zhou, H.Y., Dong, C.Y., Yin, X.Y., 2008a. New U–Pb and Hf isotopic data confirm Anshan as the oldest preserved segment of the North China Craton. American Journal of Science 308, 200–231.
Liu, Y.S., Gao, S., Kelemen, P.B., Xu, W.L., 2008b. Recycled crust controls contrasting source compositions of Mesozoic and Cenozoic basalts in the North China Craton. Geochimica et Cosmochimica Acta 72, 2349–2376.
Lu, F.X., Zheng, J.P., Li, W.P., Chen, M.H., Cheng, Z.M., 2000. The main evolution pattern of Phanerozoic mantle in the eastern China: the "mushroom cloud" model. Earth Science Frontiers 7, 97–107.
McKenzie, D., O'Nions, R.K., 1995. The source regions of oceanic island basalts. Journal of Petrology 36, 133–159.
Meng, Q.R., Zhang, G.W., 2000. Geologic framework and tectonic evolution of the Qinling orogen, central China. Tectonophysics 323, 183–196.
Menzies, M.A., Xu, Y.G., 1998. Geodynamics of the North China Craton. In: Flower, M.F.J., Chung, S.L., Lo, C.H., Lee, T.Y. (Eds.), Mantle Dynamics and Plate Interactions in East Asia. American Geophysical Union, Washington D. C., pp. 155–165.
Menzies, M.A., Fan, W.M., Zhang, M., 1993. Paleozoic and Cenozoic lithoprobes and the loss of >120 km of Archean lithosphere, Sino-Korean craton, China. In: Prichard, H.M., Alabaster, T., Harris, N.B.W., Neary, C.R. (Eds.), Magmatic Processes and Plate Tectonics. Geological Society Special Publication, London, pp. 71–81.
Menzies, M., Xu, Y.G., Zhang, H.F., Fan, W.M., 2007. Integration of geology, geophysics and geochemistry: a key to understanding the North China Craton. Lithos 96 (1–2), 1–21.
Münker, C., Weyer, S., Scherer, E., Mezger, K., 2001. Separation of high field strength elements (Nb, Ta, Zr, Hf) and Lu from rock samples for MC-ICPMS measurements. Geochemistry, Geophysics, Geosystems 2 (No. 2001GC000183).
Niu, Y.L., 2005. Generation and evolution of basaltic magmas: some basic concepts and a new view on the origin of Mesozoic–Cenozoic basaltic volcanism in Eastern China. Geological Journal of China Universities 11, 9–46.
Niu, Y.L., 2008. The origin of alkaline lavas. Science 320, 883–884.
Niu, Y.L., O'Hara, M.J., 2003. Origin of ocean island basalts: a new perspective from petrology, geochemistry and mineral physics considerations. Journal of Geophysical Research 108 (ECV 5 1–19).
Niu, Y.L., O'Hara, M.J., 2009. MORB mantle hosts the missing Eu (Sr, Nb, Ta and Ti) in the continental crust: new perspectives on crustal growth, crust–mantle differentiation and chemical structure of oceanic upper mantle. Lithos 112, 1–17.
Niu, Y.L., Waggoner, G., Sinton, J.M., Mahoney, J.J., 1996. Mantle source heterogeneity and melting processes beneath seafloor spreading centers: the East Pacific Rise 18°–19°S. Journal of Geophysical Research 101, 27711–27733.
Niu, Y.L., Wilson, M., Humphreys, E.R., O'Hara, M.J., 2011. The origin of intra-plate ocean island basalts (OIB): the lid effect and its geodynamic implications. Journal of Petrology 52, 1443–1468.
O'Reilly, S.Y., Griffin, W.L., 1988. Mantle metasomatism beneath western Victoria, Australia, part I, metasomatic processes in Cr-diopside lherzolites. Geochimica et Cosmochimica Acta 52, 433–447.
Pei, F.P., Xu, W.L., Wang, Q.H., Wang, D.Y., Lin, J.Q., 2004. Mesozoic basalt and mineral chemistry of the mantle-derived xenocrysts in Feixian, western Shandong, China: constraints on nature of Mesozoic lithospheric mantle. Geological Journal of China Universities 10 (1), 88–97.
Pei, F.P., Xu, W.L., Yang, D.B., Yu, Y., Wang, W., Zhao, Q.G., 2011. Geochronology and geochemistry of Mesozoic mafic–ultramafic complexes in the southern Liaoning and southern Jilin provinces, NE China: constraints on the spatial extent of destruction of the North China Craton. Journal of Asian Earth Sciences 40, 636–650.
Plank, T., Langmuir, C.H., 1998. The chemical composition of subducting sediment and its consequences for the crust and mantle. Chemical Geology 145, 325–394.
Rosman, K.J.R., Taylor, P.D.P., 1997. Isotopic composition of the elements. Pure and Applied Chemistry 70, 217–235.
Rudnick, R.L., Gao, S., 2003. Composition of the Continental Crust. In: Rudnick, R.L. (Ed.), Treatise on Geochemistry. The Crust. Elsevier-Pergamon, Oxford, pp. 1–64.
Rudnick, R.L., Gao, S., Ling, W.L., Liu, Y.S., McDonough, W.F., 2004. Petrology and geochemistry of spinel peridotite xenoliths from Hannuoba and Qixia, North China Craton. Lithos 77, 609–637.
Ryerson, F.J., Watson, E.B., 1987. Rutile saturation in magmas: implications for Ti–Nb–Ta depletion in island-arc basalts. Earth and Planetary Science Letters 86, 225–239.
Salters, V.J.M., Blichert-Toft, J., Fekiacova, Z., Sachi-Kocher, A., Bizimis, M., 2006. Isotope and trace element evidence for depleted lithosphere in the source of enriched Ko'olau basalts. Contributions to Mineralogy and Petrology 151, 297–312.
Santosh, M., 2010. Assembling North China Craton within the Columbia supercontinent: the role of double-sided subduction. Precambrian Research 178, 149–167.
Schmitz, M.D., Vervoort, J.D., Bowring, S.A., Patchett, P.J., 2004. Decoupling of the Lu–Hf and Sm–Nd isotope systems during the evolution of granulitic lower crust beneath southern Africa. Geology 32, 405–408.
Sengör, A.M.C., Natal'in, B.A., Burtman, V.S., 1999. Evolution of the altaid tectonic collage and Palaeozoic crustal growth in Eurasia. Nature 364, 299–307.
Song, B., Nutman, A.P., Liu, D.Y., Wu, J.S., 1996. 3800 to 2500 Ma crust in the Anshan area of Liaoning Province, northeastern China. Precambrian Research 78, 79–94.
Stracke, A., Snow, J.E., 2009. The Earth's mantle is more depleted than we thought. Eos Transactions AGU 90 (52) (Fall Meet. Supplement, V24A-03).
Sun, S.S., McDonough, W.F., 1989. Chemical and isotopic systematics of oceanic basalt: implications for mantle composition and processes. In: Saunders, A.D., Norry, M.J. (Eds.), Magmatism in the Ocean Basins. Geological Society Special Publication, London, pp. 528–548.
Tang, Y.J., Zhang, H.F., Ying, J.F., 2006. Asthenosphere–lithospheric mantle interaction in an extensional regime: implication from the geochemistry of Cenozoic basalts from Taihang Mountains, North China Craton. Chemical Geology 233, 309–327.
Taylor, S.R., McLennan, S.M., 1985. The Continental Crust: Its Composition and Evolution. Blackwell Scientific Publication, Oxford.
van Westrenen, W., Blundy, J., Wood, B., 1999. Crystal-chemical controls on trace element partitioning between garnet and anhydrous silicate melt. American Mineralogist 84, 838–847.
Vervoort, J.D., Blichert-Toft, J., 1999. Evolution of the depleted mantle: Hf isotope evidence from juvenile rocks through time. Geochimica et Cosmochimica Acta 63, 533–556.
Vervoort, J.D., Patchett, P.J., 1996. Behavior of hafnium and neodymium isotopes in the crust: constraints from Precambrian crustally derived granites. Geochimica et Cosmochimica Acta 60, 3717–3733.
Vervoort, J.D., Patchett, P.J., Blichert-Toft, J., Albarède, F., 1999. Relationships between Lu–Hf and Sm–Nd isotopic systems in the global sedimentary system. Earth and Planetary Science Letters 168, 79–99.
Vervoort, J.D., Patchett, P.J., Albarède, F., Blichert-Toft, J., Rudnick, R., Downes, H., 2000. Hf–Nd isotopic evolution of the lower crust. Earth and Planetary Science Letters 181, 115–129.
Wang, H.F., Yang, X.C., Zhu, B.Q., Fan, S.K., Dai, T.M., 1988. K–Ar chronology and evolution of the Cenozoic volcanic rocks in the eastern China. Geochimica 3, 1–11.
Wang, W., Xu, W.L., Ji, W.Q., Yang, D.B., Pei, F.P., 2006. Late Mesozoic and Paleogene basalts and deep-derived xenocrysts in eastern Liaoning province, China: constraints on nature of lithospheric mantle. Geological Journal of China Universities 12 (1), 30–40.
Wang, W., Xu, W.L., Wang, D.Y., Ji, W.Q., Yang, D.B., Pei, F.P., 2007. Caiyuanzi Paleogene basalts and deep-derived xenocrysts in eastern Liaoning, China: constraints on nature and deep process of the Cenozoic lithospheric mantle. Journal of Mineralogy and Petrology 27 (1), 63–70.
Wang, Y., Zhao, Z.F., Zheng, Y.F., Zhang, J.J., 2011. Geochemical constraints on the nature of mantle source for Cenozoic continental basalts in east-central China. Lithos 125, 940–955.
Wilde, S., Zhou, X.H., Nemchin, A.A., Sun, M., 2003. Mesozoic crust–mantle interaction beneath the North China Craton: a consequence of the dispersal of Gondwanaland and accretion of Asia. Geology 31, 817–820.
Workman, R.K., Hart, S.R., 2005. Major and trace element composition of the depleted MORB mantle (DMM). Earth and Planetary Science Letters 231, 53–72.
Wu, F.Y., Walker, R.J., Ren, X.W., Sun, D.Y., Zhou, X.H., 2003. Osmium isotopic constraints on the age of lithospheric mantle beneath northeastern China. Chemical Geology 197, 107–129.
Wu, F.Y., Lin, J.Q., Wilde, S.A., Zhang, X.O., Yang, J.H., 2005. Nature and significance of the Early Cretaceous giant igneous event in eastern China. Earth and Planetary Science Letters 233, 103–119.
Wu, F.Y., Walker, R.J., Yang, Y.H., Yuan, H.L., Yang, J.H., 2006. The chemical–temporal evolution of lithospheric mantle underlying the North China Craton. Geochimica et Cosmochimica Acta 70, 5013–5034.
Xiao, Y., Zhang, H.F., Fan, W.M., Ying, J.F., Zhang, J., Zhao, X.M., Su, B.X., 2010. Evolution of lithospheric mantle beneath the Tan–Lu fault zone, eastern North China Craton: evidence from petrology and geochemistry of peridotite xenoliths. Lithos 117, 229–246.
Xu, Y.G., 1999. Roles of thermo-mechanic and chemical erosion in continental lithospheric thinning. Bulletin of Mineralogy, Petrology and Geochemistry 18, 1–5.

Xu, Y.G., 2001. Thermo-tectonic destruction of the Archaean lithospheric keel beneath the Sino-Korean craton in china: evidence, timing and mechanism. Physics and Chemistry of the Earth, Part A: Solid Earth and Geodesy 26, 747–757.
Xu, Y.G., 2007. Diachronous lithospheric thinning of the North China Craton and formation of the Daxin'anling–Taihangshan gravity lineament. Lithos 96, 281–298.
Xu, Y.G., Ma, J.L., Frey, F.A., Feigenson, M.D., Liu, J.F., 2005. Role of lithosphere–asthenosphere interaction in the genesis of Quaternary alkali and tholeiitic basalts from Datong, western North China Craton. Chemical Geology 224, 247–271.
Xu, W.L., Gao, S., Wang, Q.H., Wang, D.Y., Liu, Y.S., 2006a. Mesozoic crustal thickening of the eastern North China Craton: evidence from eclogite xenoliths and petrologic implications. Geology 34, 721–724.
Xu, W.L., Wang, Q.H., Wang, D.Y., Guo, J.H., Pei, F.P., 2006b. Mesozoic adakitic rocks from the Xuzhou–Suzhou area, eastern China: evidence for partial melting of delaminated lower continental crust. Journal of Asian Earth Sciences 27, 230–240.
Xu, W.L., Hergt, J.M., Gao, S., Pei, F.P., Wang, W., Yang, D.B., 2008a. Interaction of adakitic melt-peridotite: implications for the high-Mg# signature of Mesozoic adakitic rocks in the eastern North China Craton. Earth and Planetary Science Letters 265, 123–137.
Xu, Y.G., Blusztajn, J., Ma, J.L., Suzuki, K., Liu, J.F., Hart, S.R., 2008b. Late Archean to early Proterozoic lithospheric mantle beneath the western North China Craton: Sr–Nd–Os isotopes of peridotite xenoliths from Yangyuan and Fansi. Lithos 102, 25–42.
Xu, W.L., Gao, S., Yang, D.B., Pei, F.P., Wang, Q.H., 2009. Geochemistry of eclogite xenoliths in Mesozoic adakitic rocks from Xuzhou–Suzhou area in central China and their tectonic implications. Lithos 107, 269–280.
Xu, W.L., Yang, D.B., Gao, S., Pei, F.P., Yu, Y., 2010. Geochemistry of peridotite xenoliths in Early Cretaceous high-Mg# diorites from the Central Orogenic Block of the North China Craton: the nature of Mesozoic lithospheric mantle and constraints on lithospheric thinning. Chemical Geology 270, 257–273.
Xu, W.L., Zhou, Q.J., Pei, F.P., Yang, D.B., Gao, S., Li, Q.L., Yang, Y.H., 2013. Destruction of the North China Craton: delamination or thermal/chemical erosion? Mineral chemistry and oxygen isotope insights from websterite xenoliths. Gondwana Research 23, 119–129.
Yang, W., Li, S.G., 2008. Geochronology and geochemistry of the Mesozoic volcanic rocks in western Liaoning: implications for lithospheric thinning of the North China Craton. Lithos 102, 88–117.
Yang, Y.H., Zhang, H.F., Xie, L.W., Liu, Y., Qi, C.S., Tu, X.L., 2006. Petrogenesis of typical Mesozoic and Cenozoic volcanic rocks from the North China Craton: new evidence from Hf isotopic studies. Acta Petrologica Sinica 22 (6), 1665–1671.
Yang, D.B., Xu, W.L., Pei, F.P., Wang, Q.H., Gao, S., 2008a. Chronology and Pb isotope compositions of Early Cretaceous adakitic rocks in Xuzhou–Huaibei area, central China: constraints on magma sources and tectonic evolution in the eastern North China Craton. Acta Petrologica Sinica 24 (8), 1745–1758.
Yang, J.H., Wu, F.Y., Wilde, S.A., Belousova, E., Griffin, W.L., 2008b. Mesozoic decratonization of the North China block. Geology 36, 467–470.
Yang, D.B., Xu, W.L., Pei, F.P., Yang, C.H., Wang, Q.H., 2012a. Spatial extent of the influence of the deeply subducted South China Block on the southeastern North China Block: constraints from Sr–Nd–Pb isotopes in Mesozoic mafic igneous rocks. Lithos 136–139, 246–260.
Yang, W., Teng, F.Z., Zhang, H.F., Li, S.G., 2012b. Magnesium isotopic systematics of continental basalts from the North China Craton: implications for tracing subducted carbonate in the mantle. Chemical Geology 328, 185–194.
Yuan, H.L., Gao, S., Luo, Y., Zong, C.L., Dai, M.N., Liu, X.M., Diwu, C.R., 2007. Study of Lu–Hf geochronology: a case study of eclogite from Dabie UHP belt. Acta Petrologica Sinica 23 (2), 232–239.
Zeng, G., Chen, L.H., Hofmann, A.W., Jiang, S.Y., Xu, X.S., 2011. Crust recycling in the sources of two parallel volcanic chains in Shandong, North China. Earth and Planetary Science Letters 302, 359–368.
Zhai, M.G., Santosh, M., 2011. The Early Precambrian odyssey of the North China Craton: a synoptic overview. Gondwana Research 20, 6–25.
Zhai, M.G., Fan, Q.C., Zhang, H.F., Sui, J.L., 2005. Lower crust processes during the lithosphere thinning in eastern China: magma underplating, replacement and delamination. Acta Petrologica Sinica 22, 1509–1526.
Zhang, H.F., 2012. Destruction of ancient lower crust through magma underplating beneath Jiaodong Peninsular, North China Craton: U–Pb and Hf isotopic evidence from granulite xenoliths. Gondwana Research 21, 281–292.
Zhang, H.F., Zheng, J.P., 2003. Geochemical characteristics and petrogenesis of Mesozoic basalts from the North China Craton: a case study in Fuxin, Liaoning Province. Chinese Science Bulletin 48 (9), 924–930.
Zhang, H.F., Sun, M., Zhou, X.H., Fan, W.M., Zhai, M.G., Ying, J.F., 2002. Mesozoic lithosphere destruction beneath the North China Craton: evidence from major-, trace-element and Sr–Nd–Pb isotope studies of Fangcheng basalts. Contributions to Mineralogy and Petrology 144, 241–253.
Zhang, H.F., Sun, M., Zhou, X.H., Zhou, M.F., Fan, W.M., Zheng, J.P., 2003. Secular evolution of the lithosphere beneath the eastern North China Craton: evidence from Mesozoic basalts and high-Mg andesites. Geochimica et Cosmochimica Acta 67, 4373–4387.
Zhang, H.F., Sun, M., Zhou, M.F., Fan, W.M., Zhou, X.H., Zhai, M.G., 2004. Highly heterogeneous late Mesozoic lithospheric mantle beneath the north China Craton: evidence from Sr–Nd–Pb isotopic systematics of mafic igneous rocks. Geological Magazine 141, 55–62.
Zhang, H.F., Zhou, X.H., Fan, W.M., Sun, M., Guo, F., Ying, J.F., Tang, Y.J., Zhang, J., Niu, L.F., 2005. Nature, composition, enrichment processes and its mechanism of the Mesozoic lithospheric mantle beneath the southeastern North China Craton. Acta Petrologia Sinica 21, 1271–1280.
Zhang, H.F., Nakamura, E., Kobayashi, K., Zhang, J., Ying, J.F., Tang, Y.J., Niu, L.F., 2007. Transformation of subcontinental lithospheric mantle through peridotite-melt reaction: evidence from a highly fertile mantle xenolith from the North China Craton. International Geology Review 49, 658–679.
Zhang, H.F., Goldstein, S., Zhou, X.H., Sun, M., Zheng, J.P., Cai, Y., 2008. Evolution of subcontinental lithospheric mantle beneath eastern China: Re–Os isotopic evidence from mantle xenoliths in Paleozoic Kimberlites and Mesozoic basalts. Contributions to Mineralogy and Petrology 155, 271–293.
Zhang, H.F., Goldstein, S.L., Zhou, X.H., Sun, M., Cai, Y., 2009a. Comprehensive refertilization of lithospheric mantle beneath the North China Craton: further Os–Sr–Nd isotopic constraints. Journal of the Geological Society 166, 249–259.
Zhang, J.J., Zheng, Y.F., Zhao, Z.F., 2009b. Geochemical evidence for interaction between oceanic crust and lithospheric mantle in the origin of Cenozoic continental basalts in east-central China. Lithos 110, 305–326.
Zhang, H.F., Ying, J.F., Tang, Y.J., Li, X.H., Feng, C., Santosh, M., 2011. Phanerozoic reactivation of the Archean North China Craton through episodic magmatism: evidence from zircon U–Pb geochronology and Hf isotopes from the Liaodong Peninsula. Gondwana Research 19, 446–459.
Zhao, G.C., Zhai, M.G., 2013. Lithotectonic elements of Precambrian basement in the North China Craton: Review and tectonic implications. Gondwana Research 23, 1207–1240.
Zhao, D., Lei, J., Tang, R., 2004. Origin of the Changbai intraplate volcano in Northeast China: evidence from seismic tomography. Chinese Science Bulletin 49, 1401–1408.
Zhao, G.C., Sun, M., Wilde, S.A., Li, S.Z., 2005. Late Archean to Paleoproterozoic evolution of the North China Craton: key issues revisited. Precambrian Research 136, 177–202.
Zheng, J.P., 1999. Mesozoic–Cenozoic Mantle Replacement and Lithospheric Thinning Beneath the Eastern China. China University of Geosciences Press, Wuhan.
Zheng, J.P., 2009. Comparison of mantle-derived materials from different spatiotemporal settings: implications for destructive and accretional processes of the North China Craton. Chinese Science Bulletin 54, 1990–2007.
Zheng, J.P., O'Reilly, S.Y., Griffin, W.L., Lu, F.X., Zhang, M., Pearson, N.J., 2001. Relict refractory mantle beneath the eastern North China block: significance for lithosphere evolution. Lithos 57, 43–66.
Zheng, J.P., Griffin, W.L., O'Reilly, S.Y., Yang, J.S., Li, T.F., Zhang, M., Zhang, R.Y., Liou, J.G., 2006. Mineral chemistry of peridotites from Paleozoic, Mesozoic and Cenozoic lithosphere: constraints on mantle evolution beneath Eastern China. Journal of Petrology 47, 2233–2256.
Zheng, J.P., Griffin, W.L., O'Reilly, S.Y., Yu, C.M., Zhang, H.F., Pearson, N., Zhang, M., 2007. Mechanism and timing of lithospheric modification and replacement beneath the eastern North China Craton: peridotitic xenoliths from the 100 Ma Fuxin basalts and a regional synthesis. Geochimica et Cosmochimica Acta 71, 5203–5225.
Zhou, X.H., 2006. Major transformation of subcontinental lithosphere beneath eastern China in the Cenozoic–Mesozoic: review and prospect. Earth Science Frontiers 13, 50–64.
Zhou, X.H., 2009. Major Transformation of Subcontinental Lithosphere beneath North China in Cenozoic–Mesozoic: revised. Geological Journal of China Universities 15, 1–18.
Zhou, X.H., Sun, M., Zhang, G.H., Chen, S., 2002. Continental crust and lithospheric mantle interaction beneath North China: isotope evidence from granulite xenoliths in Hannuoba Sino-Korean Craton. Lithos 63, 111–124.
Zhou, Z., Barrett, P.M., Hilton, J., 2003. An exceptionally preserved Lower Cretaceous ecosystem. Nature 421, 807–814.
Zindler, A., Hart, S., 1986. Chemical geodynamics. Annual Review of Earth and Planetary Sciences 14, 493–571.
Zou, H., Zindler, A., Xu, X.S., Qi, Q., 2000. Major, trace element, and Nd, Sr and Pb isotope studies of Cenozoic basalts in SE China; mantle sources, regional variations, and tectonic significance. Chemical Geology 171, 33–47.